Program Digest, 2019 IEEE International Ultrasonics Symposium (IUS)
Glasgow, Scotland, October 6-9, 2019

A Flexible Speckle Reduction Strategy using Thomson's Multitaper in High-order DMAS Beamforming

Che-Chou Shen and Pei-Ying Hsieh

Department of Electrical Engineering, National Taiwan University of Science and Technology, Taipei, Taiwan

Email: choushen@mail.ntust.edu.tw

***Abstract*—Ultrasound speckle reduction using Thomson's Multitaper is capable of improving the speckle signal-to-noise ratio (SSNR) but at the cost of image resolution. High-order Delay-Multiply-and-Sum (*p*-DMAS) beamforming can boost image resolution by *p*-th-order spatial coherence of receiving aperture. Through a tunable compounding ratio, a combination strategy of *p*-DMAS beamforming and Thomson's Multitaper is developed to provide comparable SSNR and image resolution to conventional DAS counterpart with significant improvement in image contrast (CR). Results indicate that, for *p* value of 1.5 and 1.75, the proposed Thomson's Multitaper DMAS (TM-DMAS) beamforming with optimal compounding ratio improves the image CR by 9 and 13 dB while the SSNR and image resolution remains superior or comparable to that of DAS reference.**

Keywords*—delay-multiply-and-sum, nonlinear beamforming, Thomson's multitaper, speckle reduction, high-order spatial coherence

I. Introduction

In medical ultrasound imaging, conventional delay-and-sum (DAS) beamforming shows a limited image resolution and reduced off-axis interference rejection. In order to improve the image quality in DAS beamforming, a novel nonlinear beamforming has been proposed for ultrasound imaging by multiplying received radio-frequency (RF) echoes between every possible channel pairs after time compensation. It is referred to as the delay-multiply-and-sum (DMAS) beamforming [1]. The purpose of channel-domain multiplication is to introduce the spatial coherence of receiving aperture into the beamforming process. Consequently, the side-lobe clutter and grating lobe artifacts can be suppressed in the beamforming output relative to the main-lobe signal. However, present DMAS imaging is based on the radio-frequency (RF) channel data (RF-DMAS) and thus requires large oversampling to avoid aliasing and switching of band-pass filtering to isolate the corresponding spectral components for imaging.

Inspired by the RF-DMAS beamforming, a baseband version of high-order DMAS beamforming (*p*-DMAS) is proposed using the baseband spatial coherence instead of the original RF multiplication of channel waveform [2]. Note that the *p*-DMAS does not suffer from the aforementioned requirement of oversampling and the additional band-pass filtering because no spectral up-shifting is expected in the multiplication of baseband channel data. The *p*-DMAS beamforming has been proven to manipulate the improvement in both image contrast and resolution with the flexibly tunable *p* value. However, *p*-DMAS beamforming generally exhibits a lower speckle signal-to-noise ratio (SSNR) caused by the increased speckle variation, as the speckle pattern appears more granular in the *p*-DMAS image especially with higher *p* value. In other words, the lower SSNR is the tradeoff for higher image contrast and resolution in *p*-DMAS beamforming.

Generally, methods for speckle reduction can be grouped into two categories. The first category is based on smoothing the speckle variation by averaging multiple images acquired from different spatial views (i.e., spatial compounding [3-6]). One common strategy is to steer the transmit angle into different directions and then incoherently combine these frames after image registration. Compounding can be also implemented by reconstructing the B-mode image using different spectral components and incoherently averaging these sub-band images (i.e., frequency compounding [7-8]). The second category is post-processing techniques on the B-mode image which including gabor, median, Wiener, homomorphic, or bilateral filter [9-10] or different morphological operators.

Thomson's multitaper method has recently been applied for speckle reduction in ultrasound imaging and is reported to provide satisfactory improvement of SSNR [11-12]. The tapers (i.e., apodizations) are designed to extract the highest spectral concentration from the original receiving aperture so that the main-lobe width can be better maintained for a specified spatial-frequency interval. Its implementation is based on the incoherent compounding of images with several orthogonally apodized receiving apertures but inevitably suffers from degraded image resolution due to the reduced aperture size. This paper proposes a novel combination of *p*-DMAS beamforming and Thomson's Multitaper speckle reduction method to alleviate the tradeoff of image resolution and contrast for SSNR in *p*-DMAS beamforming. Note that, since both *p*-DMAS beamforming and Thomson's Multitaper method rely on the processing of receiving aperture, they can be readily incorporated to provide improvement in image resolution, image contrast and SSNR simultaneously.

II. Theory

A. High-order DMAS beamforming (p-DMAS)

Given the baseband channel data of the *n*-th channel after phase rotation $s_n = a_n e^{j\phi_n}$ ($a_n \ge 0$) in the *N*-element array, its magnitude-square-rooted version can be constructed as $\hat{s}_n = \sqrt{a_n} e^{j\phi_n}$. In other words, the channel magnitude is scaled by taking its square root while the channel phase is kept unchanged. The proposed BB-DMAS beamforming is defined as the square of the coherent summation of the scaled channel data and can be formulated as

$$y_{\text{BB-DMAS}} = \left(\frac{1}{N} \sum_{n=1}^{N} \hat{s}_n \right)^2 \quad (1)$$

The BB-DMAS beamforming can be generalized by maintaining the channel phase but adopting the *p*-th root of the channel magnitude. After the magnitude-scaled channel data is coherently summed, the *p*-th power is performed to recover the signal dimensionality.

$$y_{p\text{-DMAS}} = \left(\frac{1}{N} \sum_{n=1}^{N} \sqrt[p]{a_n} e^{j\phi_n} \right)^p \quad (2)$$

Specifically, the generalized *p*-th root BB-DMAS beamforming uses the same signal processing for any selection of *p* value and the *p* value is no longer limited to integer value. This simplifies the implementation of BB-DMAS beamforming and also makes the manipulation of image quality much more flexible.

B. *Thomson's Multitaper*

The Thomson's Multitaper method is based on the formation of multiple orthogonal tapers, which are also known as discrete prolate spheroidal sequences (DPSS) or Slepian sequences [13]. The spatial frequency response for each taper in the Thomson's Multitaper is different so that each taper extracts different parts of the spatial spectrum of the original receiving aperture. Nonetheless, all the tapers are designed to have the highest spectral concentration and thus the main-lobe width of ultrasound beam pattern can be better maintained for a specified spatial-frequency interval after compounding. The Thomson's Multitaper can be derived using the eigenvectors of the Toeplitz matrix $D_{n,m}$:

$$D_{n,m} = \frac{\sin BW(n-m)}{\pi(n-m)}, \quad n,m = 0,1,\ldots,N-1 \quad (3)$$

where BW is the half spatial frequency interval of the main lobe after compounding in radian per sample and (n, m) are indices to form the Toeplitz matrix. N is the number of samples for each taper and thus corresponds to the number of receiving channels in the ultrasound system. Note that the number of eigenvectors with high spectral concentration increases with the spatial frequency interval BW. With the relation of $BW = 2k\pi / N$, there are $2k$ eigenvectors with high spectral concentration. Note that the spectral concentration is represented by the eigenvalue of the corresponding eigenvector. When the eigenvalue is close to one, it indicates a high spectral concentration signal.

Fig. 1 shows an example of Thomson's Multitaper together with their spatial spectrum (i.e., ultrasound beam pattern) for N=128 and k=1.5. The eigenvalues corresponding to each taper are close to one, which are 0.999, 0.969, and 0.733, respectively. We can find that each taper corresponds to different spatial spectrum.

C. *p-DMAS Beamforming with Thomson's Multitapering*

As shown in (2), the *p*-DMAS beamforming relies on magnitude scaling of time-delayed channel data by *p*-th root and restoring the output dimensionality by *p*-th power after channel sum. To incorporate the Thomson's Multitaper method into the *p*-DMAS beamforming, the magnitude-scaled channel data can be apodized by each taper and the corresponding channel sum is then envelope-detected for incoherent compounding. Moreover, in order to achieve a flexible speckle reduction, two sets of channel sum (unapodized and apodized) are used to construct the *p*-DMAS beamforming. In other words, the magnitude-scaled channel data is routed into two signal paths: one is apodized by Thomson's Multitaper while the other one remains unapodized. To combine the two unapodized and apodized channel sum for the final output of *p*-DMAS beamforming, their respective power in the stage of dimensionality restoration is modulated by a tunable compounding ratio (Cr) ranging from 0 to 1 to manipulate the extent of incoherent compounding. For example, when the compounding ratio is set to be 0.6 (i.e., 60% compounding), the apodized and unapodized channel sum contributes 60 % and 40 % respectively to the combined output of *p*-DMAS beamforming in terms of dimensionality restoration. This leads to partially apodized *p*-DMAS beamforming. After envelope detection, these partially apodized images are then eigenvalue-weighted summed to obtain the final B-mode image of *p*-DMAS beamforming with Thomson's Multitapering (TM-DMAS) as shown in the flow diagram of Fig. 2.

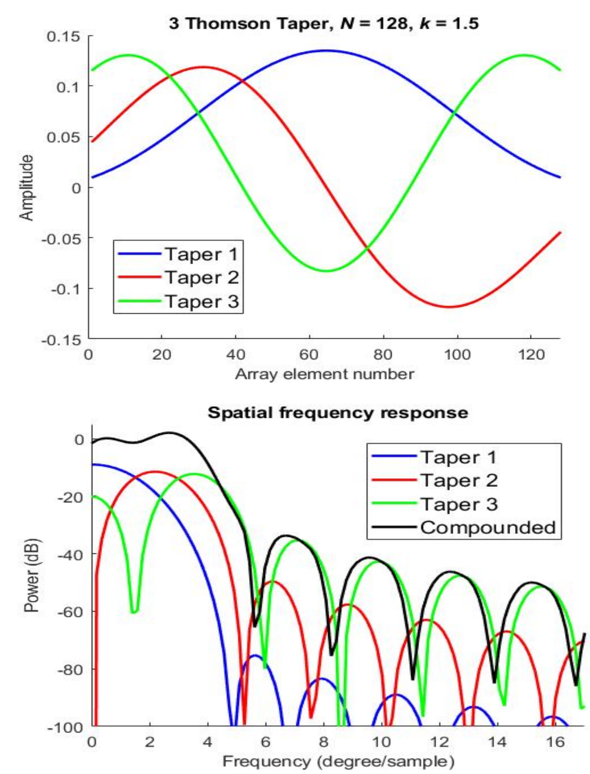

Fig. 1. The Thomson tapers for N=128 and k=1.5 and the corresponding spatial responses.

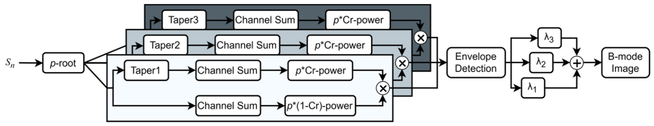

Fig. 2. Diagram of TM-DMAS beamforming.

III. Results

Experimental measurements are performed using Prodigy ultrasound imaging system (S-sharp Corporation, New Taipei City, Taiwan) with a 128-element linear array probe to acquire the pre-beamforming channel waveforms. The linear array has a pitch of 0.31 mm and a center frequency of 5 MHz. A commercial ultrasound phantom (model 549, ATS Laboratories, Bridgeport, CT. USA) was used as the imaged object. Images of the ATS phantom are acquired by setting the transmission focal depth at 30 mm using two different scanning view. One includes the anechoic cysts for evaluation of image contrast and the other contains the wire reflectors for evaluation of image resolution. In order to provide a fair comparison with tapered receiving aperture, the reference DAS image is beamformed using un-tapered (i.e., rectangular apodization) 64-channel sub-aperture in the center of the linear array. The contrast ratio (CR) and speckle signal-to-noise ratio (SSNR) are respectively calculated using the mean image values before log-compression inside the cyst (green circle) and in the background region (blue rectangle) in the upper panels of Fig. 4 and Fig. 5. On the other hand, the red rectangle in the lower panels of Fig. 4 and Fig. 5 indicates the wire at transmit focal depth for evaluation of -6-dB width in both lateral and axial directions.

Quantitative analyses of image quality as a function of compounding ratio is shown in Fig. 3. Fig. 3(a) shows the CR of TM-DMAS image with p value larger than unity is always higher than that of DAS reference for all compounding ratios. On the other hand, the SSNR of TM-DMAS beamforming in Fig. 3(b) may be inferior to that of DAS reference when a lower compounding ratio is considered. For example, when the p value is 1.5, the compounding ratio of TM-DMAS beamforming has to be higher than or equal to 0.6 to provide SSNR improvement relative to the DAS reference. Similarly, when the p value is 1.75, the TM-DMAS beamforming takes a compounding ratio of at least 0.8 to provide a comparable or even higher SSNR than the DAS reference. This observation is expectable since the extent of Thomson's Multitapering in p-DMAS beamforming increases with the compounding ratio and thus leads to more smoothed speckle and higher SSNR. For p value of 2.0, the threshold of compounding ratio to achieve SSNR improvement further increases to 1.0.

Note that, however, the increase of compounding ratio inevitably compromises the corresponding image resolution especially in the lateral direction. This is demonstrated in Fig. 3(c). Nonetheless, comparison with the DAS reference also reveals that the lateral width (LW) of TM-DMAS remains smaller than or comparable to that of DAS reference when the compounding ratio is kept lower than or equal to 0.6 and 0.8, respectively for p value of 1.5 and 1.75. Consequently, for p value of 1.5, the compounding ratio of 0.6 (i.e., 60% compounding) appears to be optimal because it simultaneously provides higher SSNR and superior image resolution than the DAS reference. Similarly, for p value of 1.75, the optimal compounding ratio can be decided to be 0.8 (i.e., 80% compounding). For p value larger than 2.0, however, there is not any compounding ratio capable of providing simultaneous improvement in both image resolution and SSNR . For the axial width (AW), however, its value appears to be relatively irrelevant to the compounding ratio in TM-DMAS beamforming as shown in Fig. 3(d). In order words, even when the TM-DMAS beamforming is applied, the corresponding axial resolution only slightly deviate from the DAS reference.

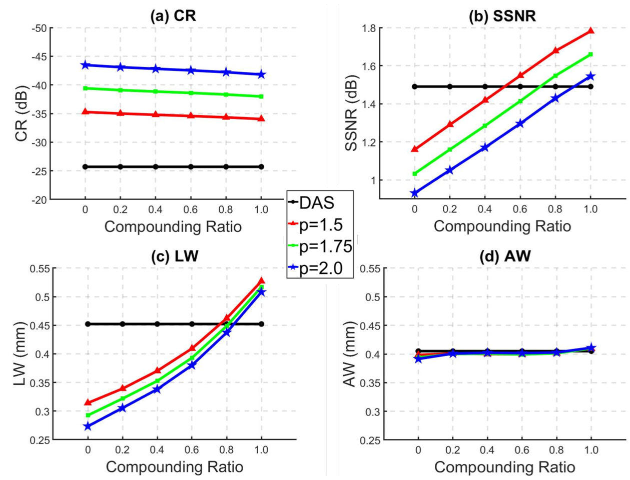

Fig. 3. Quantitative analyses of B-mode image quality as a function of compounding ratio.

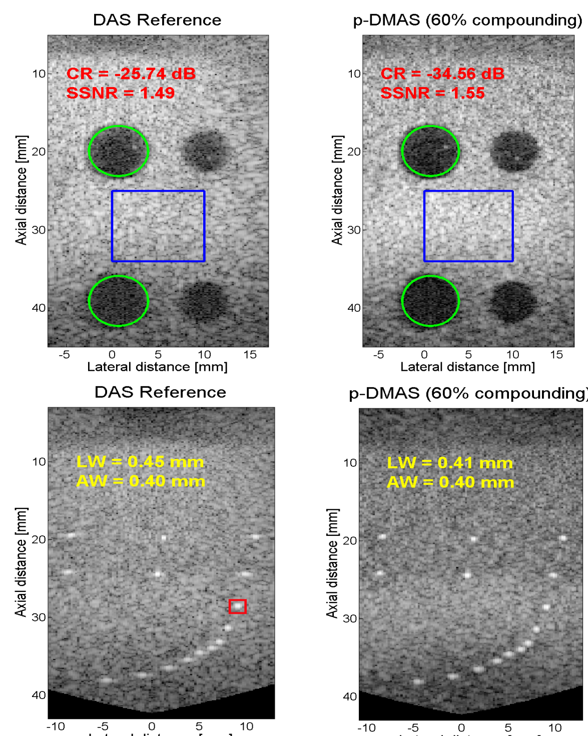

Fig. 4. Experimental B-mode images in speckle-generating phantom of DAS and TM-DMAS beamforming with p value of 1.5 and the corresponding optimal compounding ratio of 0.6.

Fig. 4 shows the experimental B-mode images of DAS reference and TM-DMAS beamforming with the p value of 1.5 and the corresponding optimal compounding ratio. For anechoic cysts in the upper panels, TM-DMAS beamforming with the optimal 60% compounding provides the CR value of -34.56 dB. This corresponds to a CR improvement of 9 dB in comparison with the CR of -25.74 dB in the DAS reference image. It should be noted that the edge of anechoic cysts are also sharpened in TM-DMAS beamforming so that the cysts can be clearly delineated. Meanwhile, the SSNR of TM-DMAS beamforming remains superior to that of DAS reference. For wire reflectors in the lower panels, the lateral width also significantly decreases from 0.45 mm of DAS reference to 0.41 mm of TM-DMAS beamforming, indicating the improvement in lateral resolution. On the other hand, the axial resolution remains almost the same between the DAS reference and the TM-DMAS beamforming.

Similarly, TM-DMAS beamforming with p value of 1.75 and the corresponding optimal 80% compounding also demonstrates a CR improvement of 13 dB from -25.74 dB in DAS reference image to -38.32 dB in TM-DMAS image in the B-mode images of anechoic cysts in the upper panels of Fig. 5. The SSNR of TM-DMAS beamforming is 1.55 which is still higher than that of DAS reference. B-mode images of wire reflectors in the lower panels of Fig. 5 also confirms that both the lateral width (LW) and axial width (AW) remains comparable to those of DAS reference when the TM-DMAS beamforming is adopted with optimal compounding ratio.

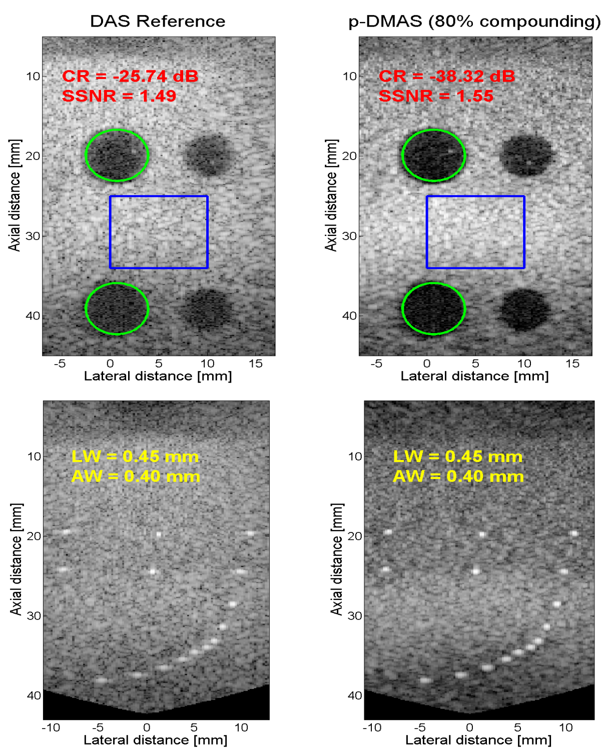

Fig. 5. Experimental B-mode images in speckle-generating phantom of DAS and TM-DMAS beamforming with p value of 1.75 and the corresponding optimal compounding ratio of 0.8.

IV. Conclusions and Discussions

In this study, the combination of Thomson's Multitaper method and high-order DMAS beamforming with a flexible compounding ratio has been proposed to effectively smooth image speckle without losing B-mode image contrast and resolution. The compounding ratio can be arbitrary selected from 0 to 1 to improve the image SSNR while the p-value of DMAS beamforming can be adjusted to recover the image quality due to compounding. Results indicate that the proposed method can outperform the DAS reference when the p-value is 1.5 and 1.75 when the corresponding optimal compounding ratio is respectively 60 % and 80 %. It seems that a higher compounding ratio is required for DMAS beamforming with higher p-value. Nonetheless, for p-value higher than 2, the proposed method appears to render inferior image SSNR to the DAS reference even with 100% compounding. Meanwhile, the corresponding image resolution also degrade to be lower than that of DAS reference.

References

[1] G. Matrone, A. S. Savoia, G. Caliano, G. Magenes, The delay multiply and sum beamforming algorithm in ultrasound B-mode medical imaging, IEEE Trans. Med. Imag. 34 (2015) 940–949.

[2] C. C. Shen, P. Y. Hsieh, Ultrasound baseband delay-multiply-and-sum (BB-DMAS) nonlinear beamforming, Ultrasonics. 96 (2019) 165–174.

[3] P.M. Shankar, Speckle Reduction in Ultrasound B-Scans Using Weighted Averaging in Spatial Compounding, IEEE Trans. Ultrason. Ferroelectr. Freq. Control 33 (1986) 754–758.

[4] S.K. Jespersen, J.E. Wilhjelm, H. Sillesen, Multi-angle compound imaging, Ultrason. Imaging, 20 (1998) 81–102.

[5] R. Entrekin, B.A. Porter, H. Sillesen, A. Wong, P. Cooperberg, C. Fix, Real-time spatial compound imaging: application to breast, vascular, and musculoskeletal ultrasound, Semin. Ultrasound CT MRI, 22 (2001) 50–64.

[6] J. Opretzka, M. Vogt, H. Ermert, A high-frequency ultrasound imaging system combining limited-angle spatial compounding and model-based synthetic aperture focusing, IEEE Trans. Ultrason. Ferroelectr. Freq. Control 58 (2011) 1355–1365.

[7] P.A. Magnin, O.T. Von Ramm, F.L. Thurstone, Frequency compounding for speckle contrast reduction in phased array images, Ultrason. Imaging, 4 (1982) 267–281.

[8] B. Mesurolle, T. Helou, M. El-Khoury, M. Edwardes, E.J. Sutton, E. Fau Kao, Tissue harmonic imaging, frequency compound imaging, and conventional imaging, J. Ultrasound Med., 26 (2007) 1041–1051.

[9] J. S. Ullom, M. Oelze, J. R. Sanchez, Ultrasound speckle reduction using coded excitation, frequency compounding, and postprocessing despeckling filters, Proc. IEEE Ultrason. Symp. (2010).

[10] R. G. Dantas, E. T. Costa, Ultrasound speckle reduction using modified gabor filters, IEEE Trans. Ultrason. Ferroelectr. Freq. Control 54 (2007) 530–538.

[11] A. C. Jensen, S. P. Nasholm, C. C. Nilsen, A. Austeng, S. Holm, Applying Thomson's multitaper approach to reduce speckle in medical ultrasound imaging, IEEE Trans. Ultrason. Ferroelectr. Freq. Control 59 (2012) 2178–2185.

[12] M. Toulemonde, O. Basset, P. Tortoli, C. Cachard, Thomson's multitaper approach combined with coherent plane-wave compounding to reduce speckle in ultrasound imaging, Ultrasonics. 56 (2015) 390–398.

[13] D. Slepian, Prolate spheroidal wave functions, Fourier analysis and uncertainty, Bell Syst. Tech. J. 57 (1978) 1371–1429.